CDF/PUB/EXOTIC/PUBLIC/7126

Search for New Particle $X \to b\bar{b}$ Produced in Association with $W^{\pm}$ Bosons at $\sqrt{s} = 1.96$ TeV

The CDF Collaboration
URL http://www-cdf.fnal.gov
(Dated: July 30, 2004)

We present searches for new particles decaying into $b\bar{b}$ and produced in association with $W^{\pm}$ bosons in $p\bar{p}$ collisions at $\sqrt{s} = 1.96$ TeV. The searches focus on the Standard Model Higgs or technicolor particle decaying into $b\bar{b}$ using approximately 162 pb^{-1} of the dataset accumulated by the updated Collider Detector at Fermilab. Events with an electron or muon, missing E_T and two jets, one of them b-tagged, are selected. The number of tagged events and the dijet mass distribution are consistent with the Standard Model expectations and we set a 95% confidence level upper limit on the production cross section times branching ratio as a function of the new particle masses. The sensitivity of the present searches is limited by statistics to a cross section approximately one order of magnitude higher than the predicted cross section for the Standard Model Higgs boson production, but is getting close to some of theoretical cross section for technicolor particle production.

Preliminary Results for Summer 2004 Conferences

I. INTRODUCTION

This note summarizes searches for new particles decaying into $b\bar{b}$ and produced in association with $W^{\pm}$ bosons in $p\bar{p}$ collisions at $\sqrt{s} = 1.96$ TeV. The search signature considered here is $W^{\pm}X$ with $W^{\pm} \to e\nu$ or $\mu\nu$, and $X \to b\bar{b}$, giving final states with one high p_T lepton, large missing E_T ($\not\!\!E_T$) and two b jets. In this note we assume X is either the Standard Model Higgs boson [1] or a new particle responsible for the dynamics of a new interaction such as Technicolor [2]. We focus our attention on the $W^{\pm} + 2$ jets signature using b tagging since it contains most of the signal, while b-tagged $W^{\pm} + \geq 3$ jets events are dominated by $t\bar{t}$ decays. Figure 1 shows the Feynman diagrams of $p\bar{p} \to W^{\pm}X \to \ell\nu b\bar{b}$ with a production cross section of the order of 0.1 pb to 5 pb.

The CDF detector is described in detail in [3].

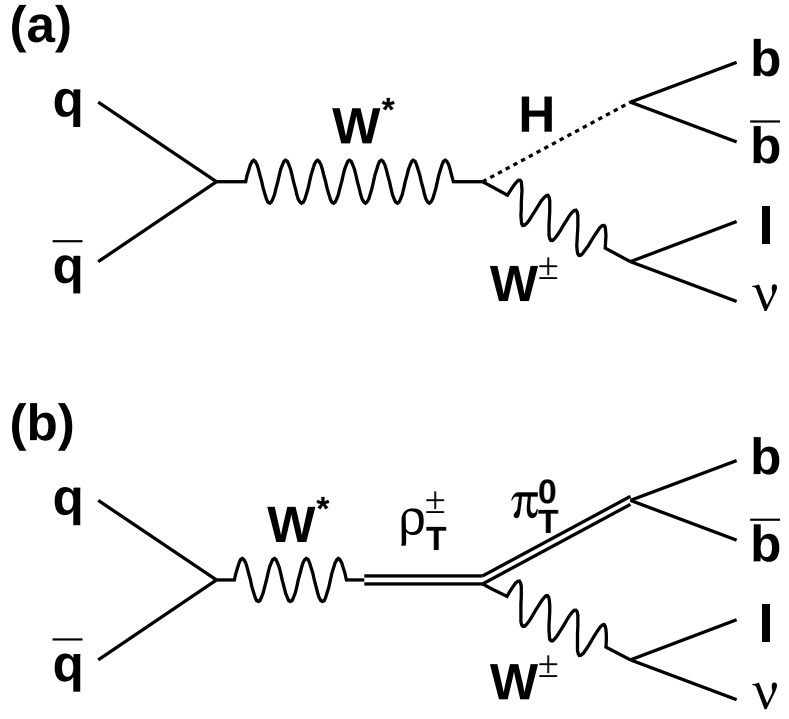

FIG. 1: The Feynman diagrams of (a)$p\bar{p} \to W^* \to W^{\pm}H \to \ell\nu b\bar{b}$ and (b)$p\bar{p} \to W^* \to \rho_T^{\pm} \to W^{\pm}\pi_T^0 \to \ell\nu b\bar{b}$.

II. DATA SAMPLE & EVENT SELECTION

This analysis is based on an integrated luminosity of 162 pb^{-1} collected with the CDFII detector between March 2002 and August 2003. The data are collected with an inclusive lepton trigger that requires an electron or muon with E_T >18 GeV (p_T >18 GeV/c for the muon). From this inclusive lepton dataset we select events offline with a reconstructed isolated electron E_T (muon p_T) greater than 20 GeV, $\not\!\!E_T$ >20 GeV, and 2 jets with E_T >15 GeV and $|\eta| < 2$.

The dataset selected above, called "lepton+jets", is dominated by QCD production of W bosons with multiple jets. To improve the signal to background we require at least one jet in the event to be identified as a heavy flavor jet by the SECVTX b-tagging algorithm [4] [5].

In order to further reduce the top contributions, we remove events with a high p_T isolated track ($p_T^{seed} > 20$ GeV/c) and charge opposite to the primary lepton. The track isolation is defined as $p_T^{seed}/(p_T^{seed} + \Sigma p_T) > 0.9$ where p_T^{seed} is the seed track p_T and Σp_T is the sum of track p_T (> 0.5 GeV/c) in a cone of radius 0.4 around the seed track. We also require that there are no any extra jets with $E_T > 8$ GeV in the forward region ($2.0 <| \eta |< 3.0$) or two more extra jets with $E_T > 8$ GeV and $E_T < 15$ GeV in the central region ($| \eta |< 2.0$).

A. Optimization

We optimize the 1st and 2nd leading jet E_T selection criteria by evaluating a significance for each set of cuts. The significance is defined as $S/\sqrt{B}$, where S is the number of signals and B is the number of backgrounds in a mass window ($\pm 1.5\sigma$). Figure 2 shows the significance as a function of the jet E_T selection criteria. Since the significance is not sensitive to the 1st leading jet E_T, we require the 1st leading jet $E_T > 15$ GeV and the 2nd leading jet $E_T > 15$ GeV, to be the same ones used in the lepton + jets analysis [5].

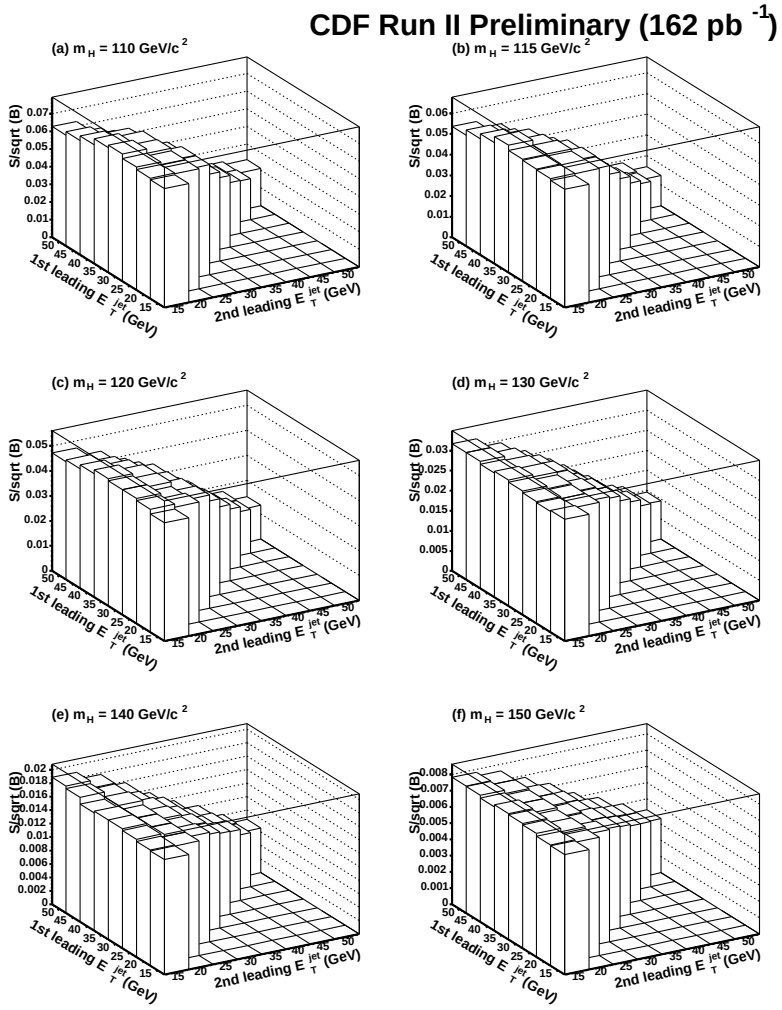

FIG. 2: The significance as a function of 1st and 2nd leading jet E_T selection criteria, which is not sensitive to the 1st leading jet E_T.

III. BACKGROUNDS

The dominant background for this analysis is QCD production of W-boson plus multijet events. These events enter the signal sample when either one of the jets is a b-jet, or a light quark jet is mis-identified as a heavy flavor jet. Mistags are estimated by parameterizing the rate of negative tags [5] in the generic QCD multi-jets sample, as a function of jet E_T, track multiplicity, η, ϕ, and the summed E_T of all the jets in the event. To first order, negative tags are a good approximate of positive mistags, since mistags are mostly due to symmetric resolution effects; however, we need to increase the negative tags rate by a factor of 1.2 ± 0.1 to account for the presence of long lived particles and secondary interactions with the detector material, contributing asymmetrically to the positive tags. These predicted tagging rates are then applied to the pretag sample. In order to evaluate the background due to W+heavy flavor, we

use ALPGEN Monte Carlo [6] to estimate the heavy flavor fraction of the inclusive W+jets events which has been calibrated using the generic QCD jets. Estimates of the tagged background are then obtained by multiplying the tagging efficiencies and the number of observed W events in the pretag sample.

The $t\bar{t}$ and single top contributions are estimated using PYTHIA [7] Monte Carlo and the NLO production cross section [8] [9].

The other substantial background in this analysis comes from events without W bosons. These events are typically QCD jet events where one jet has faked a high-p_T lepton and mismeasured energies produce apparent missing E_T. We measure this "non-W" background by extrapolating the number of tagged events with an isolated lepton and low missing E_T into the signal region of large missing E_T.

Other, small backgrounds from a variety of sources are estimated using the Monte Carlo.

The number of observed tagged events along with the expected backgrounds as a function of jet multiplicity are summarized Table I and Figure 3. We find good agreement between data and background expectations in all jet multiplicity bins.

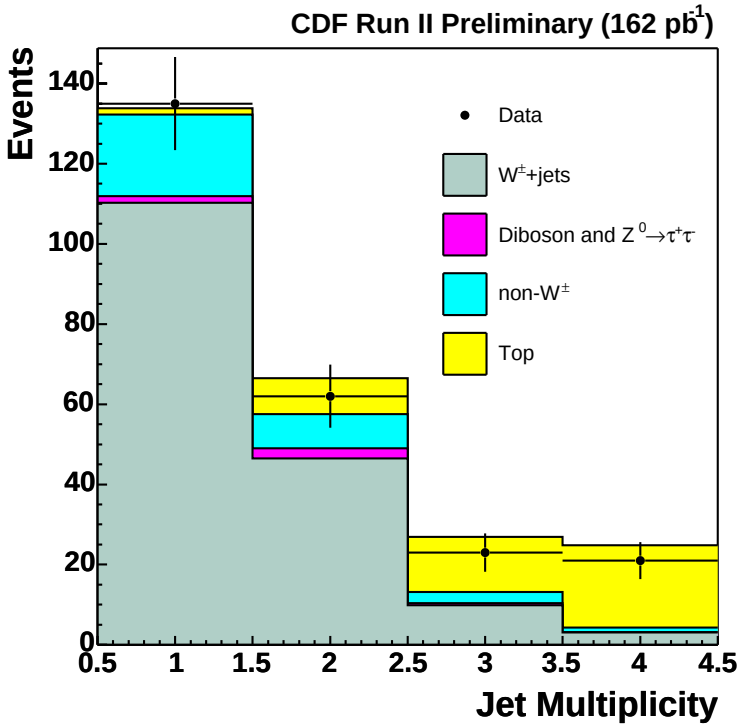

FIG. 3: The number of observed positive tagged events and the background summary as a function of jet multiplicity.

IV. RESULTS FOR THE STANDARD MODEL HIGGS SEARCH

A. WH Acceptance

The acceptance for identifying $W^{\pm}H \to \ell\nu b\bar{b}$ events is calculated from a combination of data and PYTHIA Monte Carlo samples of $p\bar{p} \to W^{\pm}H \to W^{\pm}b\bar{b}$ events as a function of the Higgs boson mass (m_H) using the cuts described above. The total acceptance is calculated as a product of the kinematic and geometric acceptance, the lepton ID efficiencies, the trigger efficiencies, the b-tagging efficiencies. A 11% systematic uncertainty comes from uncertainties in the modeling of initial (3%) and final (6%) state radiations, the parton distribution function (2%), the jet energy scale (3%), the b-tag efficiency (6%), jet energy resolution(1%), the electron and muon trigger efficiencies ($< 1\%$), and the electron and muon ID efficiencies (5%). The acceptance increases linearly from $1.5 \pm 0.2\%$ to $1.7 \pm 0.2\%$ as m_H increases from 110 to 150 GeV/c^2, shown in Figure 4.

Background	$W^{\pm}$ + 1 jet	$W^{\pm}$ + 2 jets	$W^{\pm}$ + 3 jets	$W^{\pm}$ + $\geq$ 4 jets
Events before tagging	13417	2072	313	82
mistags	36.2 ± 7.1	14.1 ± 2.6	4.0 ± 0.9	2.0 ± 0.5
$W^{\pm} + b\bar{b}$	32.2 ± 10.2	19.1 ± 5.8	3.7 ± 1.1	0.7 ± 0.2
$W^{\pm} + c\bar{c}$	11.9 ± 3.5	6.8 ± 2.2	1.2 ± 0.4	0.2 ± 0.1
$W^{\pm} + c$	30.0 ± 8.0	6.5 ± 1.8	1.0 ± 0.3	0.1 ± 0.0
Diboson/$Z^0 \to \tau^+\tau^-$	1.7 ± 0.6	2.5 ± 0.6	0.5 ± 0.1	0.1 ± 0.0
QCD	20.3 ± 2.0	8.5 ± 1.2	2.8 ± 0.5	1.1 ± 0.2
$t\bar{t}$	0.4 ± 0.1	5.1 ± 1.0	12.8 ± 2.4	20.3 ± 3.7
single top	1.2 ± 0.2	3.8 ± 0.5	0.9 ± 0.1	0.2 ± 0.0
Total Background	133.9 ± 17.5	66.5 ± 9.0	26.9 ± 3.2	24.8 ± 3.8
Observed positive tags	135	62	23	21

TABLE I: The number of observed positive tagged events and the background summary for an integrated luminosity of 162 pb^{-1}.

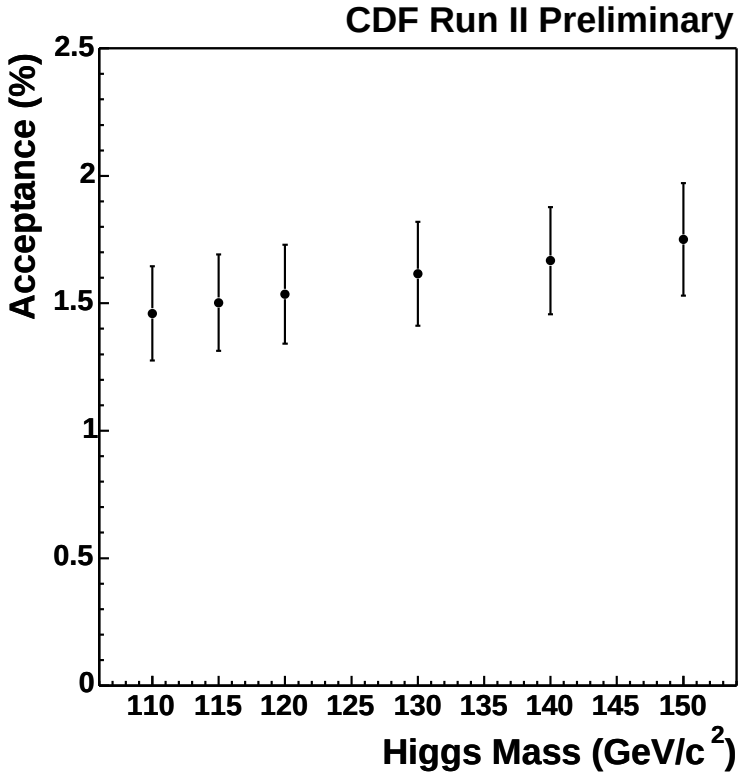

FIG. 4: The total $W^{\pm}H \to \ell\nu b\bar{b}$ acceptance as a function of the Higgs boson mass.

B. 95% C.L. Upper Limit

We perform a direct search for a resonant mass peak in the reconstructed dijet invariant mass distribution. Figure 5 shows the dijet mass distribution in the data along with the background expectations. The Standard Model Higgs signal times 10 is also shown. Since there is no mass peak as expected from the Higgs boson, we set an upper limit on the production cross section times branching ratio of $p\bar{p} \to W^{\pm}H$ as a function of m_H by using the number of events in the $W^{\pm} + 2$ jets sample.

We assume the dijet mass distribution in the data to be consistent of QCD (mistags, $W^{\pm} + b\bar{b}$, $W^{\pm} + c\bar{c}$, $W^{\pm} + c$ and diboson), TOP ($t\bar{t}$ and single top) and $W^{\pm}H$ events. A binned maximum likelihood technique is used to estimate the number of $W^{\pm}H$ signal events by constraining the number of QCD and TOP events to the expectation within

the statistical and systematic uncertainties. The expected number of events (μ) in each mass bin is

$$\mu = f_{QCD} \cdot N_{QCD} + f_{TOP} \cdot N_{TOP} + f_{W^{\pm}H} \cdot (\varepsilon \cdot \mathcal{L} \cdot \sigma_{W^{\pm}H} \cdot \mathrm{Br}\ (H \to b\bar{b})),$$

where f_{QCD}, f_{TOP} and $f_{W^{\pm}H}$ are the expected fraction of events in a given mass bin predicted by Monte Carlo and N_{QCD}, N_{TOP}, ε, $\mathcal{L}$ and $\sigma_{W^{\pm}H}$ are the expected number of QCD and TOP events, the detection efficiency, the luminosity and the unknown $W^{\pm}H$ cross section, respectively. The corresponding likelihood is

$$L = \prod_{i=bin} \frac{\mu_i^{N_i} \cdot e^{-\mu_i}}{N_i!},$$

where N_i is the observed events from $W^{\pm} + 2$ jets sample.

Figure 6 shows the 95% C.L. upper limit as a function of m_H. The cross section of the Standard Model Higgs and the Technicolor process ($p\bar{p} \to W^{\pm}\pi_T^0$) is also included for comparison.

Figure 7 shows the pseudo experiment results. The measurement is consistent with the pseudo experiment results. Although we have a much improved limit over the Run 1 [10], the sensitivity of the present search is limited by statistics to a cross section approximately one order of magnitude higher than the predicted cross section for the Standard Model Higgs boson production.

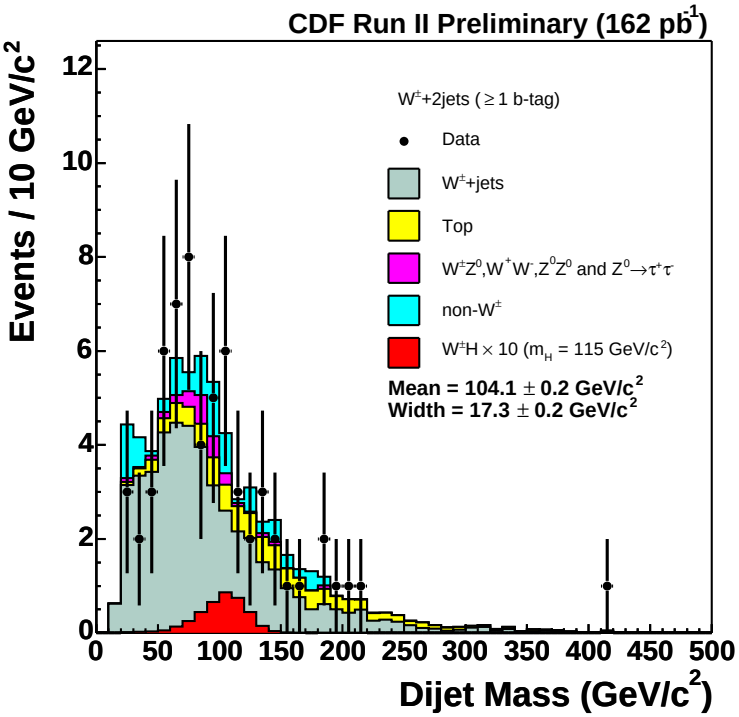

FIG. 5: The dijet mass distribution in the data along with the background expectations and the scaled Higgs boson mass (115 GeV/c^2) distribution by a factor of 10.

C. Cross Checks

1. *Pretag Dijet Mass Distributions*

As a cross check, we have compared the pretag dijet mass distribution with the expectation from the various backgrounds, which are shown in Figure 8. The agreement between data and MC is quite good, which gives us confidence towards our detector simulation and background calculations.

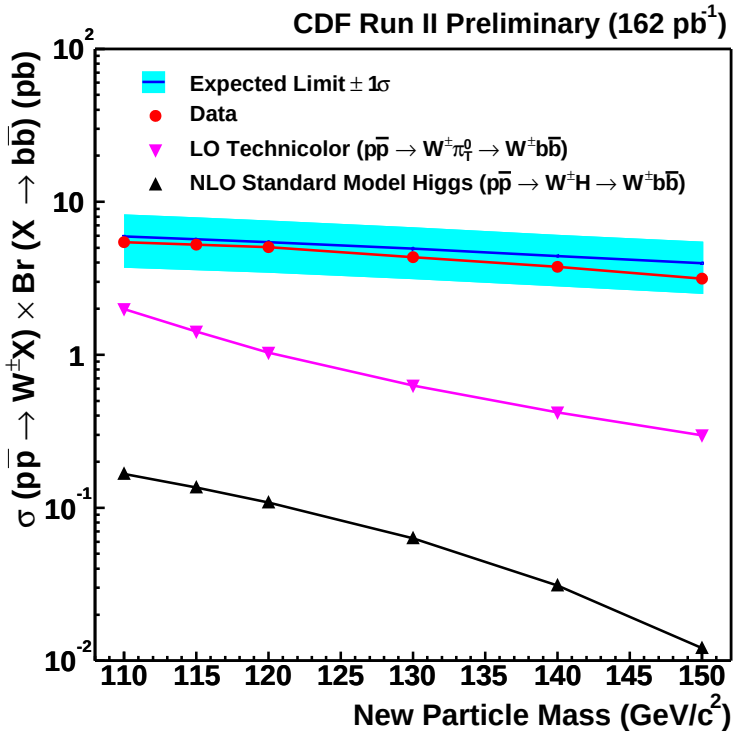

FIG. 6: The 95% C.L. upper limit (red circle) on the $W^{\pm}H$ cross section as a function of the Higgs boson mass. Also shown is the theoretical cross section (black triangle) for the production of a Standard Model Higgs boson in association with a $W^{\pm}$ boson, and the pseudo experiment results (blue line). As for the comparison, the production cross section of the Technicolor process ($p\bar{p} \to W^{\pm}\pi_T^0$) is also included (purple triangle).

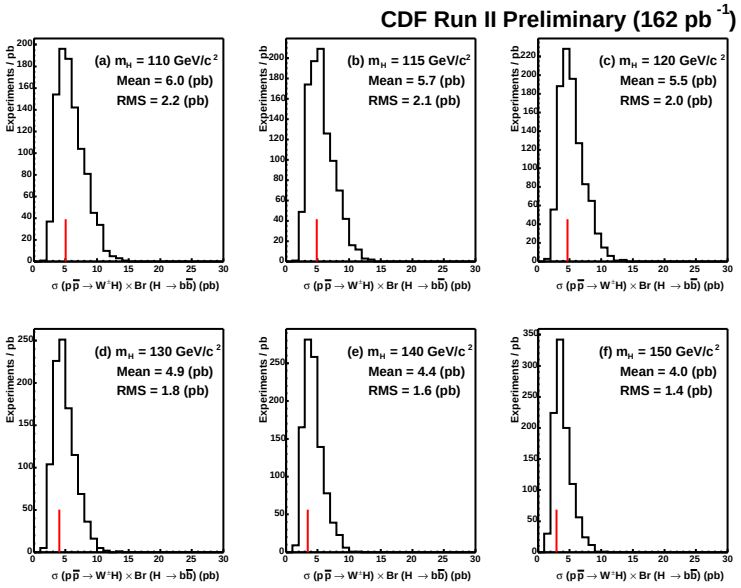

FIG. 7: The pseudo experiment results. The red line shows the results from data.

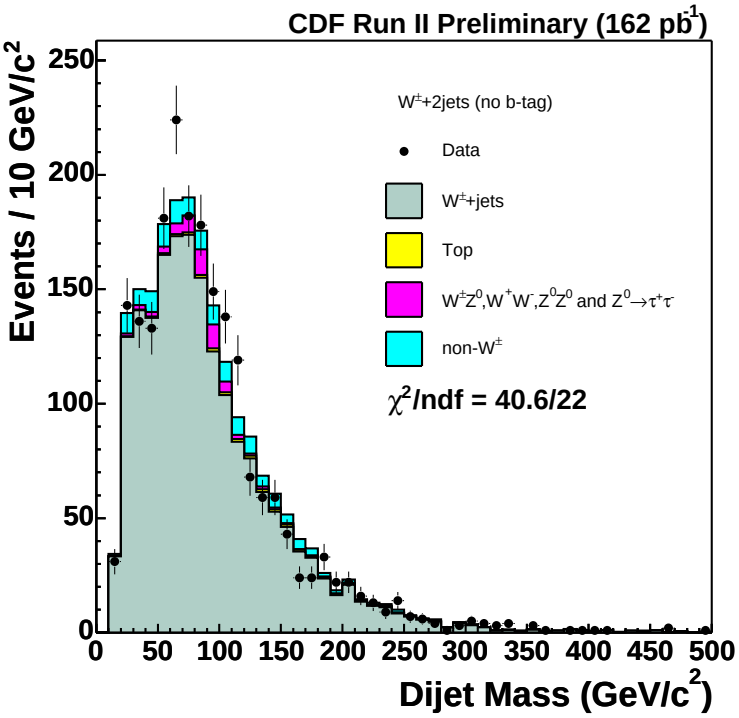

FIG. 8: The dijet mass distribution before tagging.

2. *Significance Comparison*

We compared the significance with the Run 1 and the Higgs sensitivity report ones [11–13]. The results are shown in Table II. The significance of this analysis is in line between the Run 1 and the Run2 Higgs sensitivity studies with current detector configuration, so called "CASE 0", without extension to higher η for either lepton identification or b-tagging.

	Run2	Run1		Run2 Higgs sensitivity report	
	This Analysis	Cut Based	NN	CASE 0	
Mass Resolution	17%	15%		15%	10%
S	0.24	0.31	0.24	0.13	0.13
B	18.1	50.7	18.3	3.2	2.1
$S/\sqrt{B}$	0.057	0.04	0.056	0.075	0.09

TABLE II: The significance comparison of different analysis. The "CASE 0" in the Run2 Higgs sensitivity report uses the same lepton selection and SECVTX b-tagging as this analysis. There is no extension of higher η for either lepton identification or b-tagging. Both jets are required to be b-tagged, but allowing the second b-tag to be significantly looser (SECVTX or JPB) than the first one (SECVTX).

V. RESULTS FOR TECHNICOLOR PARTICLE SEARCH ($p\bar{p} \to \rho_T^{\pm} \to W^{\pm}\pi_T^0$)

A. $\rho_T^{\pm} \to W^{\pm}\pi_T^0$ Acceptance

The acceptance for identifying $\rho_T^{\pm} \to W^{\pm}\pi_T^0 \to \ell\nu b\bar{b}$ events is calculated from a combination of data and PYTHIA Monte Carlo samples of $p\bar{p} \to \rho_T^{\pm} \to W^{\pm}\pi_T^0 \to W^{\pm}b\bar{b}$ events as a function of $m(\rho_T^{\pm})$ and $m(\pi_T^0)$ using the same

cuts as Higgs search. The total acceptance is calculated as a production of the kinematic and geometric acceptance, the lepton ID efficiency, the trigger efficiency, the b-tagging efficiency, and various scale factors to account for the differences between data and Monte Carlo. A 12% systematic uncertainty comes from uncertainties in the modeling of initial (4%) and final (7%) state radiations, the parton distribution function (2%), the jet energy scale (3%), the b-tag efficiency (6%), jet energy resolution (1%), the electron and muon trigger efficiencies ($< 1\%$), and the electron and muon ID efficiencies (5%). The acceptance increases linearly from $0.9 \pm 0.2\%$ to $1.5 \pm 0.2\%$ as $m(\rho_T^{\pm})$ and $m(\pi_T^0)$ increase, shown in Figure 9.

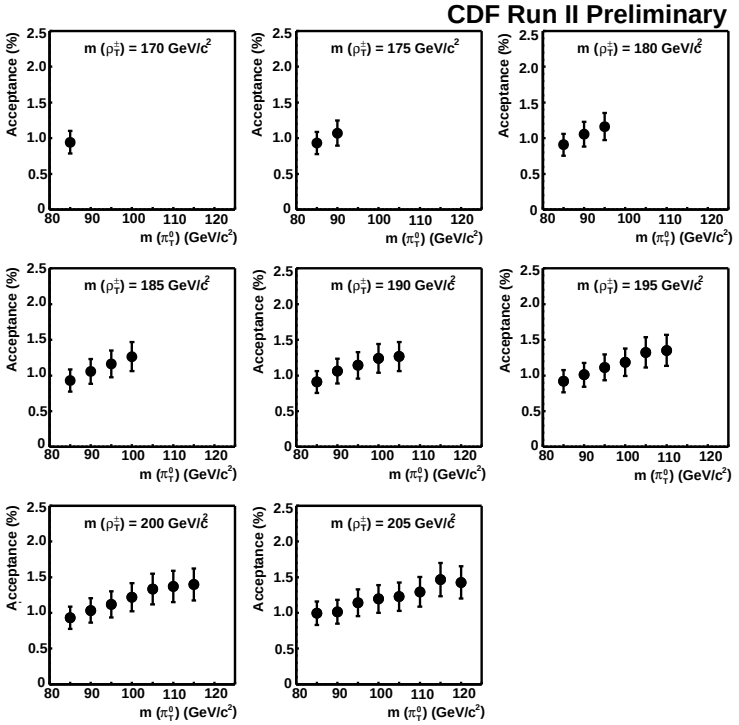

FIG. 9: The total $\rho_T^{\pm} \to W^{\pm}\pi_T^0 \to \ell\nu b\bar{b}$ acceptance as a function of technipion mass ($m(\pi_T^0)$).

B. 95% C.L. Upper Limit

We perform a direct search for a mass peak in the reconstructed $W^{\pm} + 2$ jets and dijet invariant mass distributions.

To reconstruct the $W^{\pm} + 2$ jets mass, we need to determine the p_z of neutrino from $W^{\pm}$ boson. We use the $W^{\pm}$ mass constraint in the lepton-neutrino system and take the smaller p_z if there are two solutions. If there is no solution for p_z, we take the real part of the solution of the quadratic equation.

Figures 10 and 11 show the $W^{\pm} + 2$ jets and dijet mass distributions. Since there is no mass peak observed from $\rho_T^{\pm}$ and π_T^0, we set an upper limit on the production cross section times branching ratio of $p\bar{p} \to \rho_T^{\pm} \to W^{\pm}\pi_T^0$ as a function of $m(\rho_T^{\pm})$ and $m(\pi_T^0)$ by using the number of events in the $W^{\pm} + 2$ jets sample. A 2-dimensional binned maximum likelihood technique, similar to the one described in Sec. IV B, is used to estimate the number of $\rho_T^{\pm} \to W^{\pm}\pi_T^0$ signal events by constraining the number of QCD and TOP events to the expectation within the statistical and systematic uncertainties.

Figure 12 show the mass correlation between the $W^{\pm}$+ 2jets mass and the dijet mass from the $W^{\pm} + 2$ jets data, QCD, TOP, and $\rho_T^{\pm} \to W^{\pm}\pi_T^0 \to \ell\nu b\bar{b}$. The advantage of the 2-dimensional likelihood is to treat the mass correlation properly.

Figure 13 (14) shows the 95% C.L. upper limit and the pseudo experiment results as a function of $m(\pi_T^0)$ ($m(\rho_T^{\pm})$) for different $m(\rho_T^{\pm})$ ($m(\pi_T^0)$). The sensitivity of the present search is still limited by statistics, but is getting close to some of theoretical cross section, as shown in Figure 15 for the ratio of measured cross section limit and PYTHIA prediction in the $\rho_T^{\pm}$ and π_T^0 mass plane.

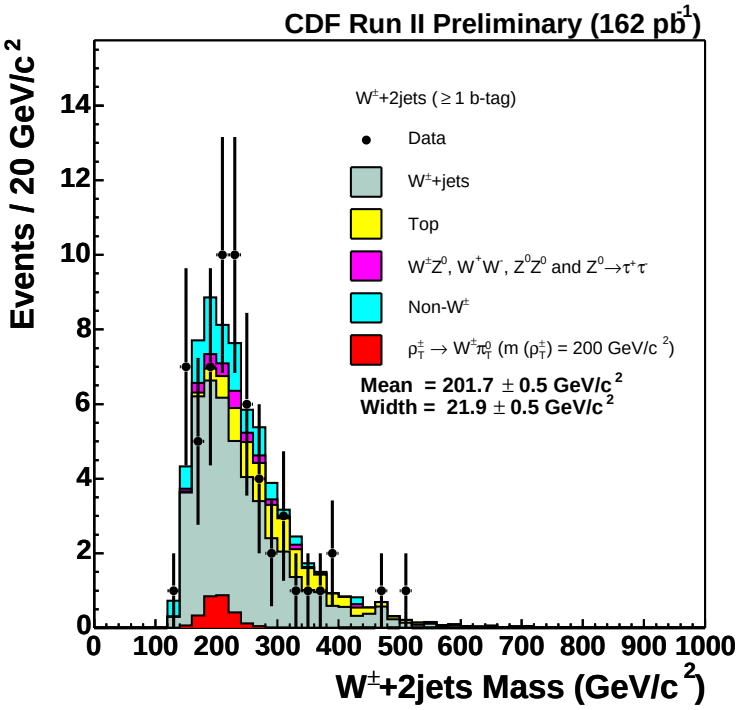

FIG. 10: The $W^{\pm}+2$ jets mass distribution in the data along with the backgrounds and signal expectations.

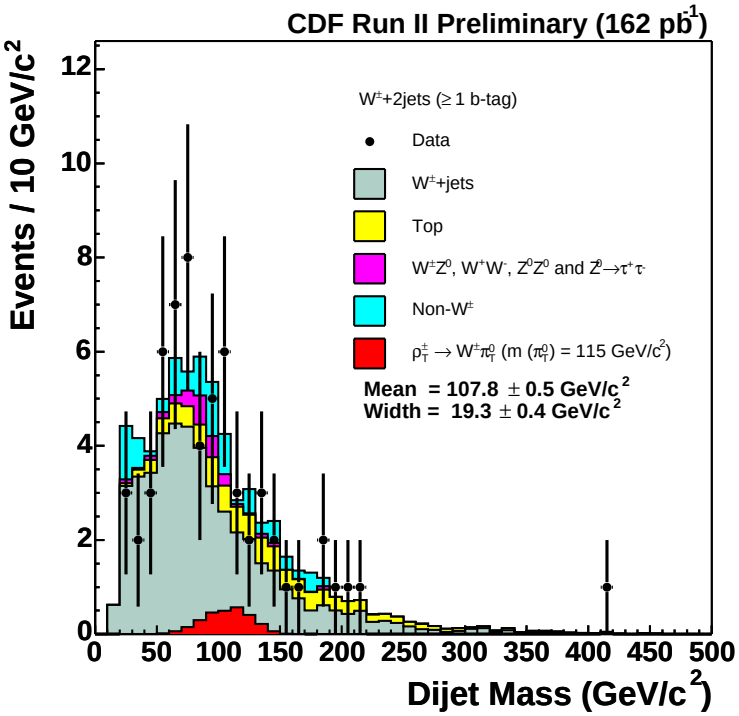

FIG. 11: The dijet mass distribution in the data along with the backgrounds and signal expectations.

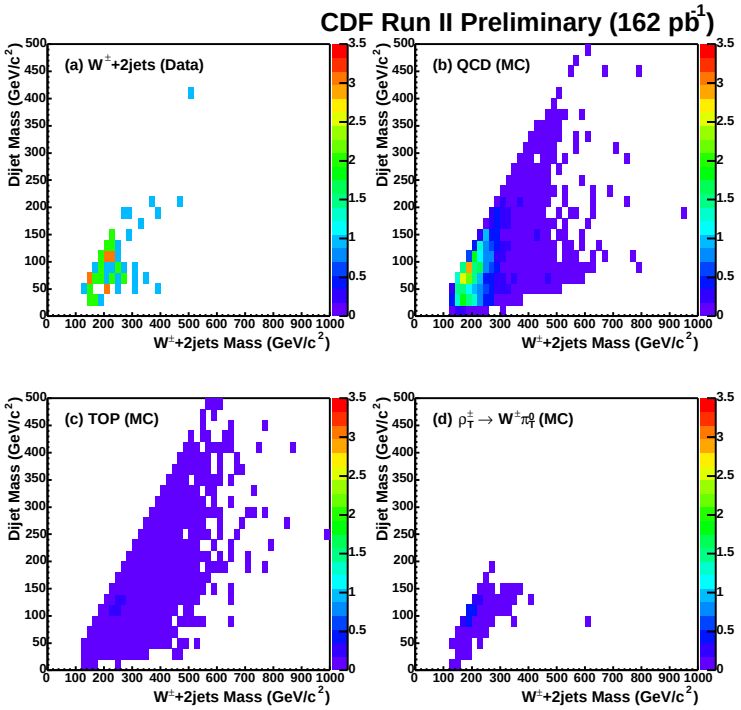

FIG. 12: The dijet mass vs $W^{\pm}+2$ jets mass distribution. (a)$W^{\pm}+2$ jets (Data), (b)QCD background (MC), (c)TOP background (MC), (d)$\rho_T^{\pm} \to W^{\pm}\pi_T^0$ (MC).

VI. CONCLUSION

We performed a search for new particles decaying into $b\bar{b}$ and produced in association with a $W^{\pm}$ boson at the Run 2 dataset. The dijet mass spectrum shows no significant excess of events in the b-tagged $W^{\pm}+2$ jet events. We set a 95% C.L. upper limit on the production cross section times branching ratios as a function of new particle mass. The sensitivity of the present search is limited by statistics to a cross section approximately one orders of magnitude higher than the predicted cross section for the Standard Model Higgs boson production, but is getting close to some of theoretical cross section for technicolor particle production. We should be able to either discover these new technicolor particles or exclude them in the near future.

Acknowledgments

We thank the Fermilab staff and the technical staffs of the participating institutions for their vital contributions. This work was supported by the U.S. Department of Energy and National Science Foundation; the Italian Istituto Nazionale di Fisica Nucleare; the Ministry of Education, Culture, Sports, Science and Technology of Japan; the Natural Sciences and Engineering Research Council of Canada; the National Science Council of the Republic of China; the Swiss National Science Foundation; the A.P. Sloan Foundation; the Bundesministerium fuer Bildung und Forschung, Germany; the Korean Science and Engineering Foundation and the Korean Research Foundation; the Particle Physics and Astronomy Research Council and the Royal Society, UK; the Russian Foundation for Basic Research; the Comision Interministerial de Ciencia y Tecnologia, Spain; and in part by the European Community's Human Potential Programme under contract HPRN-CT-20002, Probe for New Physics.

[1] J. Gunion et al. "The Higgs Hunter's Guide" (Addison-Wesley; New York, 1990)
[2] K. Lane and S. Mrenna, Phys. Rev. D **67**, 115011 (2003).

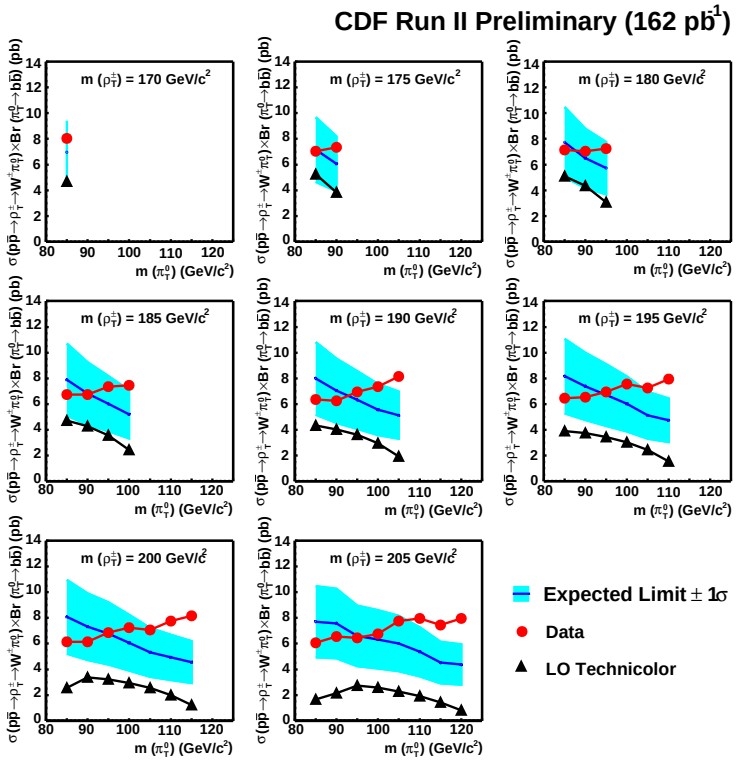

FIG. 13: The 95% C.L. upper limit (red circle) on the $\rho_T^{\pm} \to W^{\pm}\pi_T^0$ cross section as a function of $m(\pi_T^0)$ for different $m(\rho_T^{\pm})$. Also shown is the theoretical cross section (black triangle) for the production of $\rho_T^{\pm} \to W^{\pm}\pi_T^0$, and the pseudo experiment results (blue line).

[3] F. Abe, et al., Nucl. Instrum. Methods Phys. Res. A **271**, 387 (1988); D. Amidei, et al., Nucl. Instum. Methods Phys. Res. A **350**, 73 (1994); F. Abe, et al., Phys. Rev. D **52**, 4784 (1995); P. Azzi, et al., Nucl. Instrum. Methods Phys. Res. A **360**, 137 (1995); The CDFII Detector Technical Design Report, Fermilab-Pub-96/390-E

[4] T. Affolder, et al., Phys. Rev. D **64**, 032002 (2001).

[5] D. Acosta, et al., Measurement of the $t\bar{t}$ Production Cross Section in $p\bar{p}$ collisions at $\sqrt{s}$=1.96 TeV using Lepton + Jets Events with Secondary Vertex b-tagging, PRD in preparation.

[6] M.L. Mangano et al., JHEP **07**, 1 (2003).

[7] T. Sjostrand et al., High-Energy-Physics Event Generation with PYTHIA 6.1, Comput. Phys. Commun. **135**, 238 (2001).

[8] M. Cacciari et al., JHEP **404** 68(2004).

[9] T. Stelzer et al., Phys. Rev. D **56**, 5919 (2002).

[10] F. Abe, et al. Phys. Rev. Lett. **79**, 3819 (1997).

[11] C. Neu, A Search for the Higgs Boson in Proton - Antiproton Collisions at $\sqrt{s} = 1.8$ TeV, PhD Thesis at OSU (2003).

[12] M. Carena *et al.*, Report of the Tevatron Higgs Working Group, hep-ph/0010338.

[13] CDF and DØ Collaborations, Results of the Tevatron Higgs Sensitivity Study, FERMILAB-PUB-03/320-E.

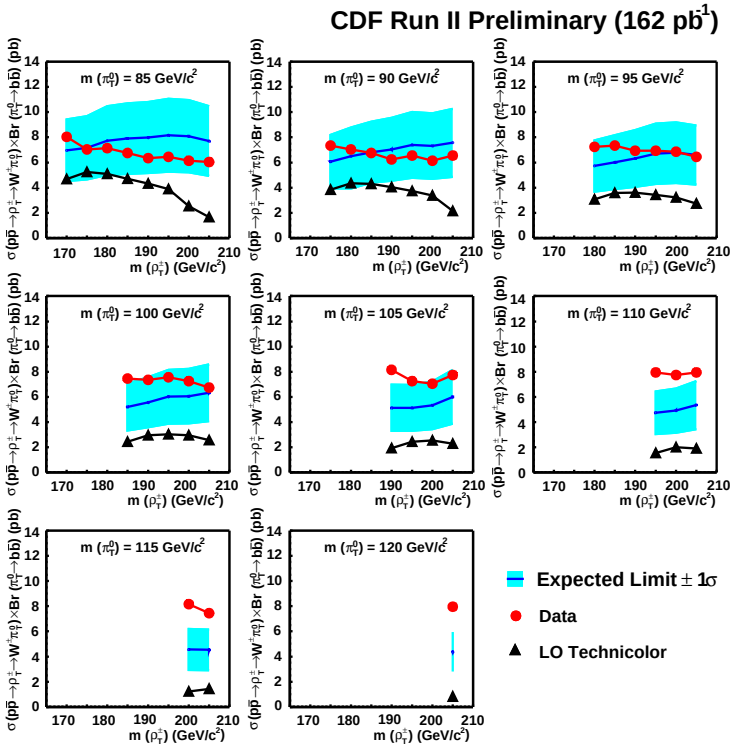

FIG. 14: The 95% C.L. upper limit (red circle) on the $\rho_T^{\pm} \to W^{\pm}\pi_T^0$ cross section as a function of $m(\rho_T^{\pm})$ for different $m(\pi_T^0)$. Also shown is the theoretical cross section (black triangle) for the production of $\rho_T^{\pm} \to W^{\pm}\pi_T^0$, and the pseudo experiment results (blue line).

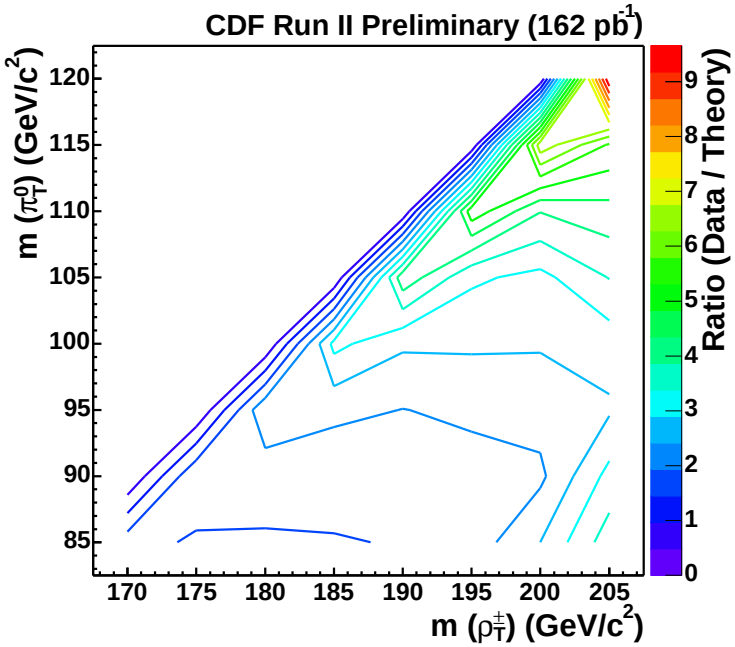

FIG. 15: The ratio of measured 95% C.L. upper limit and pythia predictions for the $p\bar{p} \to \rho_T^{\pm} \to W^{\pm}\pi_T^0$ cross section is ploted in contour as color coded in the $\rho_T^{\pm}$ and π_T^0 mass plane.